Knudsen effusion mass spectrometric determination of the complex vapor composition of samarium, europium, and ytterbium bromides

ARTICLE *in* RAPID COMMUNICATIONS IN MASS SPECTROMETRY · AUGUST 2013

Impact Factor: 2.25 · DOI: 10.1002/rcm.6617 · Source: PubMed

5 AUTHORS, INCLUDING:

Dmitry N. Sergeev
Forschungszentrum Jülich
18 PUBLICATIONS **28** CITATIONS
SEE PROFILE

Mikhail Fyodorovich Butman
Ivanovo State University of Chemistry and …
78 PUBLICATIONS **324** CITATIONS
SEE PROFILE

Vladimir Motalov
Ivanovo State University of Chemistry and …
44 PUBLICATIONS **142** CITATIONS
SEE PROFILE

L. S. Kudin
Ivanovo State University of Chemistry and …
100 PUBLICATIONS **405** CITATIONS
SEE PROFILE

Research Article

Rapid Communications in Mass Spectrometry

Received: 15 February 2013 Revised: 1 April 2013 Accepted: 29 April 2013 Published online in Wiley Online Library

Rapid Commun. Mass Spectrom. **2013**, 27, 1715–1722
(wileyonlinelibrary.com) DOI: 10.1002/rcm.6617

Knudsen effusion mass spectrometric determination of the complex vapor composition of samarium, europium, and ytterbium bromides

D. N. Sergeev[1], M. F. Butman[1], V. B. Motalov[2]*, L. S. Kudin[2] and K. W. Krämer[3]

[1]Department of Technology of Ceramics and Nanomaterials, Ivanovo State University of Chemistry and Technology, Ivanovo 153000, Russia
[2]Department of Physics, Ivanovo State University of Chemistry and Technology, Ivanovo 153000, Russia
[3]Department of Chemistry and Biochemistry, University of Bern, CH-3012 Bern, Switzerland

RATIONALE: The vaporization of Sm, Eu, and Yb tri- and dibromides is accompanied by decomposition and disproportionation reactions. These result in complex vapor compositions whose analysis is an intricate problem for experimentalists. Approaches have been developed to interpret mass spectra and accurately determine the vapor composition of thermally unstable compounds.
METHODS: A sector type magnet instrument was used. A combined ion source allowed the study of both the molecular and ionic vapor compositions in the electron ionization (EI) and the thermionic emission (TE) modes. The methodological approaches were based on a joint analysis of the ionization efficiency functions, the temperature and time dependences of the ion currents, and special mathematical data evaluation.
RESULTS: The vaporization of $SmBr_3$, $YbBr_3$, $SmBr_2$, $EuBr_2$, and $YbBr_2$ was studied in the temperature range of 850–1300 K. An initial stage of incongruent vaporization was observed in the case of the tribromides, $SmBr_2$, and $YbBr_2$. This eventually changed to a congruent vaporization stage. Various neutral (Ln, Br, Br_2, LnBr, $LnBr_2$, $LnBr_3$, Ln_2Br_4, Ln_2Br_5, and Ln_2Br_6) and charged (Br^-, $LnBr_3^-$, $LnBr_4^-$) species were detected at different vaporization stages.
CONCLUSIONS: The quantitative vapor composition of Sm, Eu, and Yb tri- and dibromides was determined. It was found that only $EuBr_2$ was stable in the studied temperature range. The developed approaches can be useful in the case of other thermally unstable compounds. Copyright © 2013 John Wiley & Sons, Ltd.

It is known that most lanthanide (Ln) tribromides vaporize congruently.[1–3] Their vapor contains predominantly monomeric molecules $LnBr_3$, a small fraction (1–10%) of dimer molecules Ln_2Br_6, and a negligibly small amount of larger oligomers (trimers, tetramers, etc.), as well as negative ions $(LnBr_3)_nBr^-$ ($n = 0$–4). In contrast, Sm, Eu, and Yb tribromides decompose partly or completely at high temperatures by the reaction:

$$2LnBr_3(s) \rightarrow 2LnBr_2(s) + Br_2(g) \quad (1)$$

In addition, the vapor composition can be more complex and time dependent.[4,5] This is also the case for the dibromides of Sm, Eu, and Yb which tend to disproportionate at high temperatures by the reaction:

$$3LnBr_2(s) \rightarrow Ln(s) + 2LnBr_3(s) \quad (2)$$

Unfortunately, reactions (1) and (2) were not taken into account in earlier investigations[6,7] on the vaporization of Sm and Yb bromides by torsion effusion. The authors assumed that the vapor consisted mainly of $LnBr_3$ molecules in the case of tribromides and $LnBr_2$ molecules in the case of dibromides. Such assumptions are not justified and may lead to large uncertainties in the derived thermodynamic parameters, e.g. sublimation enthalpies. Therefore, Knudsen effusion mass spectrometry (KEMS) should be used to monitor *in situ* the changes in the vapor composition of these compounds.

In the present work we investigate the vaporization of thermally unstable Sm, Eu, and Yb di- and tribromides by KEMS and establish the occurrence of neutral and charged vapor species under disproportionation/decomposition conditions.

EXPERIMENTAL

Knudsen effusion experiments with mass spectrometric analysis of vapor species were carried out at Ivanovo State University of Chemistry and Technology (Ivanovo, Russia). A MI1201 magnetic sector-type (angle of 90°, curvature radius of 200 mm) mass spectrometer was used. It was supplied by JSC "SELMI" (Sumy, Ukraine) and modified by us for high-temperature studies. A special ion source allowed measurements in the electron ionization (EI) and the thermal ion emission (TE) regimes and the study of both neutral and charged vapor components. In the EI regime, the molecular composition of the equilibrium vapor

* *Correspondence to:* V. B. Motalov, Department of Physics, Ivanovo State University of Chemistry and Technology, Ivanovo 153000, Russia.
E-mail: v.motalov@gmail.com

was analyzed over the condensed phase. Mass spectra of the molecular beam from the Knudsen effusion cell were recorded using 50 eV ionizing electrons and a cathode emission current of 1 mA. A movable molecular beam shutter, positioned between the effusion cell and the ionization chamber, made it possible to distinguish the species effusing from the cell from those of the background. In the TE regime, the charged species were identified. In this case, ions were generated inside the effusion cell at a high temperature and drawn out by a weak (10^4–10^5 V/m) electric field. The voltage applied to the cell was negative with respect to the ground in order to detect the emission of negative ions. The detection system for the ion current included a secondary electron multiplier combined with a picoammeter (Keithley, Cleveland, OH, USA). The sensitivity for the direct current was 10^{-17} A. The sample under investigation was loaded into a graphite or molybdenum cell. The ratio of the cross-sectional area of the cell to the area of the effusion orifice (0.16 mm^2) was about 300. The cell was heated by a resistance oven. The cell temperature was measured by a standard tungsten-rhenium thermocouple calibrated by the melting points of pure NaBr and Ag. The accuracy of the temperature measurement is estimated to be within ±5 K. The instrument was calibrated with metallic silver as internal standard. An automatic program module[8] recorded the ion current, the cell temperature, and the energy of the ionizing electrons. A more detailed description of the unit and the experimental procedure was given earlier.[9]

The $LnBr_3$ (Ln = Sm, Yb) samples were synthesized from the respective oxides Ln_2O_3 (99.9%; Fluka, Buchs, Switzerland) following the NH_4Br route.[10,11] It includes the dissolution of the oxide in concentrated (47%) HBr acid, the addition of NH_4Br, the formation of the ternary ammonium rare earth bromide, and its decomposition to $LnBr_3$ by heating in vacuum. For further purification, the dry $LnBr_3$ powders were sublimed in vacuum.

The $EuBr_2$ sample was synthesized from Eu_2O_3 (99.9%, Fluka). By the procedure described above, a mixture of $EuBr_2$ and $EuBr_3$ was obtained, which was then decomposed to pure $EuBr_2$ by further annealing at 773 K in vacuum.

The $LnBr_2$ (Ln = Sm, Yb) samples were obtained by a synproportionation reaction from $LnBr_3$ and the Ln metal (99.99%, Metall Rare Earth Ltd, Sheung Shui, Hong Kong, China).[12] The metal was used in small excess in a $LnBr_3$/Ln ratio of 2:1.05 to ensure a complete reduction to the divalent state. The reactions were carried out in welded tantalum containers enclosed in silica ampoules. The quality of all the samples was proven by powder X-ray diffraction. All patterns contained reflections of the respective phase only. $SmBr_3$[13] and $YbBr_3$[14] crystallized in the $PuBr_3$ and BiI_3 structure types, respectively. At room temperature, $SmBr_2$[15] and $EuBr_2$[16] adopt the $SrBr_2$ structure type and $YbBr_2$[17] shows the SrI_2 structure type.

RESULTS AND DISCUSSION

Mass spectra and ionization efficiency curves

Ytterbium and samarium tribromides

In the Yb and Sm tribromide vaporization experiments two main stages relating to the different temperature ranges were observed (denoted by I and II in Figs. 1 and 2, and

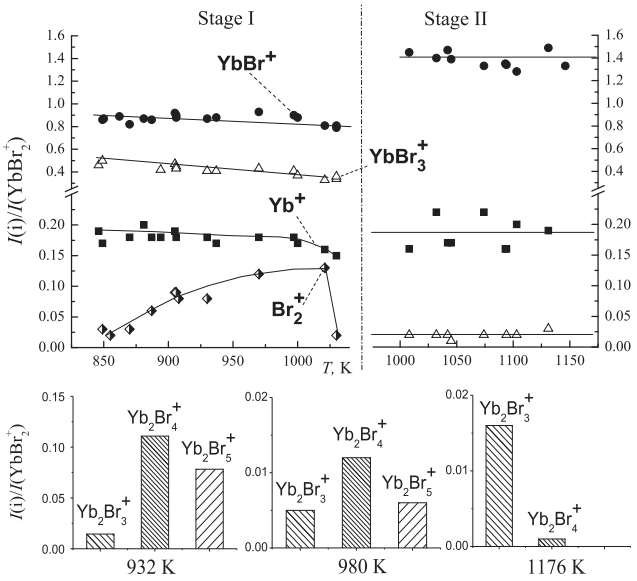

Figure 1. Temperature dependences of the EI mass spectra upon the vaporizations of $YbBr_3$.

Table 1). The experimental data at stage I (Figs. 1 and 2) were obtained by a step-by-step heating; at each short isothermal delay the mass spectra were recorded. At this stage the vaporization was incongruent due to the decomposition reaction (1) which is evident due to the presence of Br^+ and Br_2^+ ions in the mass spectra. Because of effusion bromine depletion of the system occurred. Reaction (1) was naturally accelerated with temperature unless an irreversible transition to stage II took place. At this stage the Br_2^+ and Br^+ ions vanished completely from the mass spectra and the vaporization demonstrated congruency in the heating/cooling cycles up to the end of experiment. Note that these and all subsequent data were obtained from a graphite cell for which stage I lasted longer at the same temperature than in a

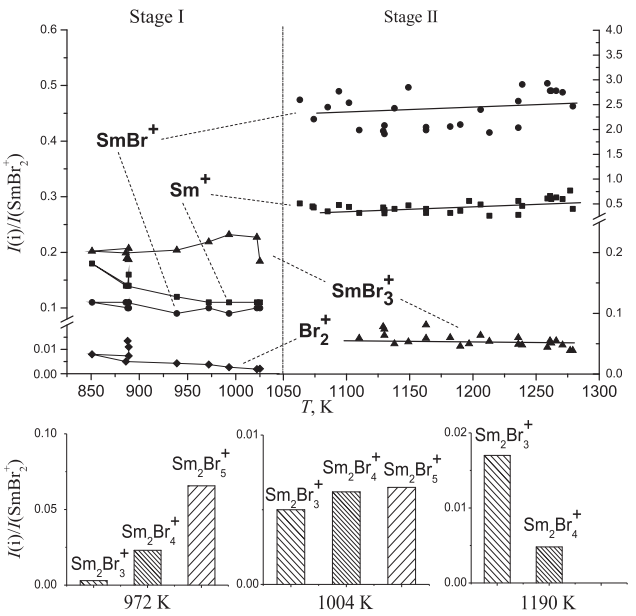

Figure 2. Temperature dependences of the EI mass spectra upon the vaporizations of $SmBr_3$.

Rapid Communications in Mass Spectrometry

Table 1. EI mass spectra for 50 eV and vapor compositions

Sample	Vaporization stage, temperature [K]	Ion species in EI mass spectra (relative ion currents)	Relative vapor compositions (%)	
			Neutral species	Ions
$YbBr_3$	Stage I: 850–1050	Yb^+(18), $YbBr^+$(91), $YbBr_2^+$(100), $YbBr_3^+$(42), Br^+(54), Br_2^+(10), $Yb_2Br_3^+$(1.4), $Yb_2Br_4^+$(11.1), $Yb_2Br_5^+$(7.8)	$YbBr_3$(39.1), $YbBr_2$(11.7), Br(35.2), Br_2(5.9), Yb_2Br_4(0.6), Yb_2Br_5(4.3), Yb_2Br_6(3.1)	$YbBr_4^-$(99.9), $YbBr_3^-$(0.1)
	Stage II: 1000–1250	Yb^+(18), $YbBr^+$(139), $YbBr_2^+$(100), $YbBr_3^+$(2), $Yb_2Br_3^+$(1.6), $Yb_2Br_4^+$(0.1)	$YbBr_2$(95.2),$YbBr_3$(3.8), YbBr(0.5), Yb_2Br_4(0.48), Yb_2Br_5(0.02);	$YbBr_4^-$(83.3) $YbBr_3^-$(16.7)
$SmBr_3$	Stage I: 850–1050	Sm^+(13), $SmBr^+$(10), $SmBr_2^+$(100), $SmBr_3^+$(20), Br^+(19), Br_2^+(0.5), $Sm_2Br_3^+$(0.3), $Sm_2Br_4^+$(2.3), $Sm_2Br_5^+$(6.6)	$SmBr_3$(57.8), $SmBr_2$(2.3), Br(36.4), Br_2(1.2), Sm_2Br_4(0.1), Sm_2Br_5(0.6), Sm_2Br_6(1.7);	$SmBr_4^-$
	Stage II: 1050–1300	Sm^+(46), $SmBr^+$(246), $SmBr_2^+$(100), $SmBr_3^+$(6), $Sm_2Br_3^+$(1.7), $Sm_2Br_4^+$(0.5)	$SmBr_2$(91.6), $SmBr_3$(8.2), Sm_2Br_4(0.1), Sm_2Br_5(0.1);	$SmBr_4^-$(83.3), $SmBr_3^-$(16.7)
$YbBr_2$	960–1300	Yb^+(19), $YbBr^+$(126), $YbBr_2^+$(100), $YbBr_3^+$(2), $Yb_2Br_3^+$(1.6), $Yb_2Br_4^+$(0.1)	$YbBr_2$(94.32),Yb(0.94), YbBr(0.47), $YbBr_3$(3.77), Yb_2Br_4(0.47), Yb_2Br_5(0.02);	$YbBr_4^-$(83.3), $YbBr_3^-$(16.7)
$SmBr_2$	1060–1300	Sm^+(48), $SmBr^+$(305), $SmBr_2^+$(100), $SmBr_3^+$(3), $Sm_2Br_3^+$(1.3), $Sm_2Br_4^+$(0.3)	$SmBr_2$(94.04), $SmBr_3$(4.70), SmBr(0.94), Sm(0.14), Sm_2Br_4(0.14), Sm_2Br_5(0.04);	$SmBr_4^-$(80), $SmBr_3^-$(20)
$EuBr_2$	1049–1261	Eu^+(46), $EuBr^+$(238), $EuBr_2^+$(100), $Eu_2Br_3^+$(2)	$EuBr_2$(99.2), Eu(0.05), EuBr(0.3), Eu_2Br_4(0.45)	$EuBr_3^-$

molybdenum cell. As can be seen in Figs. 1 and 2 and Table 1, the mass spectra differed considerably for the different stages. At both stages, the mass spectra differed from those of the lanthanide tribromides.[18–20] The phenomena that stand out in particular are a very high fraction of $LnBr^+$ ions and a wide variety of ions containing two lanthanide atoms.

In order to determine the molecular precursors of the ions at each vaporization stage, we recorded the ionization efficiency curves (IECs), which show the dependence of the mass spectra on the energy of the ionizing electrons. IECs for the Ln^+, $LnBr^+$, $LnBr_2^+$, $LnBr_3^+$, and Br_2^+ ions were measured in the course of one experiment and normalized for a fixed electron energy (4–5 eV above the threshold; see Figs. 3 and 4). The energy scale in Figs. 3 and 4 was calibrated using the ionization energy of molecular bromine; $I_0(Br_2) = 10.517 \pm 0.003$ eV.[21] It should be noted that the ion appearance energies were not determined precisely in this work, because such a determination from the superimposed spectra of the individual molecules is complicated. For the interpretation of the mass spectra, we therefore focus on the analysis of the shapes of the IECs.

It can be seen from Fig. 3 that the shapes of the IECs for Yb^+ and $YbBr_2^+$ ions differ substantially for the temperature ranges of 877–988 K and 1067–1174 K that correspond to the different stages of vaporization (Fig. 1). It is obvious to draw the conclusion that at stage I (877–988 K) these ions are mainly formed from the $YbBr_3$ molecules. In addition, the low-energy tails extending to about 15 eV (Yb^+) and 9 eV ($YbBr_2^+$) demonstrate the presence of $YbBr_2$ molecules. These dominate in the vapor of stage II (1067–1174 K). At this stage the intensities of the $YbBr_3^+$ ions were too low for IEC measurements. Note that the $YbBr_3^+$ ions are exclusively formed from $YbBr_3$ molecules, in agreement with previous reports on other $LnBr_3$ molecules.[18–20] However, the shape of the IEC of the $YbBr^+$ ions at stage II changes only insignificantly compared with those of the Yb^+ and $YbBr_2^+$ ions. This observation can be explained if the $YbBr_2$ molecules are the main precursor for the $YbBr^+$ ions at any stage of vaporization. In addition, the low-energy tail, which appears on the $YbBr^+$ IEC at 1067–1174 K, indicates some contribution from YbBr molecules.

A similar analysis was performed for the IECs of samarium-containing ions (Fig. 4). In contrast to $YbBr^+$, the $SmBr^+$ ions are mainly formed from $SmBr_3$ molecules at stage I and from $SmBr_2$ at stage II. The larger amount of tribromide molecules at stage I is evidence for the higher thermodynamic stability of $SmBr_3$ than of $YbBr_3$, and *vice versa* the higher stability of $YbBr_2$ than of $SmBr_2$. In addition, no low-energy tail is observed for the $SmBr^+$ curve, i.e. there are no SmBr molecules in the vapor, thus providing support for this conclusion.

The variation of the fractions of two Ln atoms containing ions at the different vaporization stages (see Figs. 1 and 2) correlates with the respective $LnBr_3$ and $LnBr_2$ contributions to the ion currents. This observation allows the $Ln_2Br_3^+$, $Ln_2Br_4^+$, and $Ln_2Br_5^+$ ion currents to be attributed to the Ln_2Br_4, Ln_2Br_5, and Ln_2Br_6 molecules.

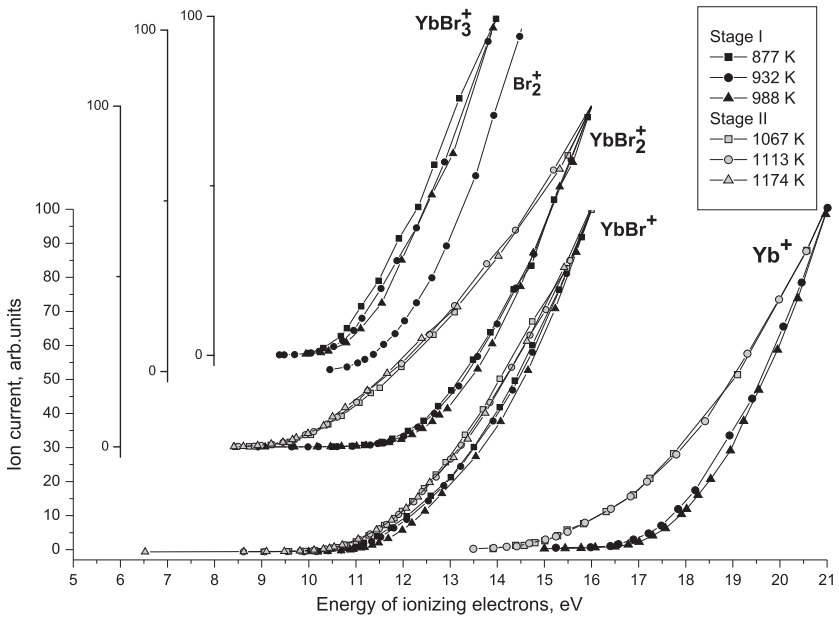

Figure 3. Ionization efficiency curves at stages I and II of vaporization of $YbBr_3$.

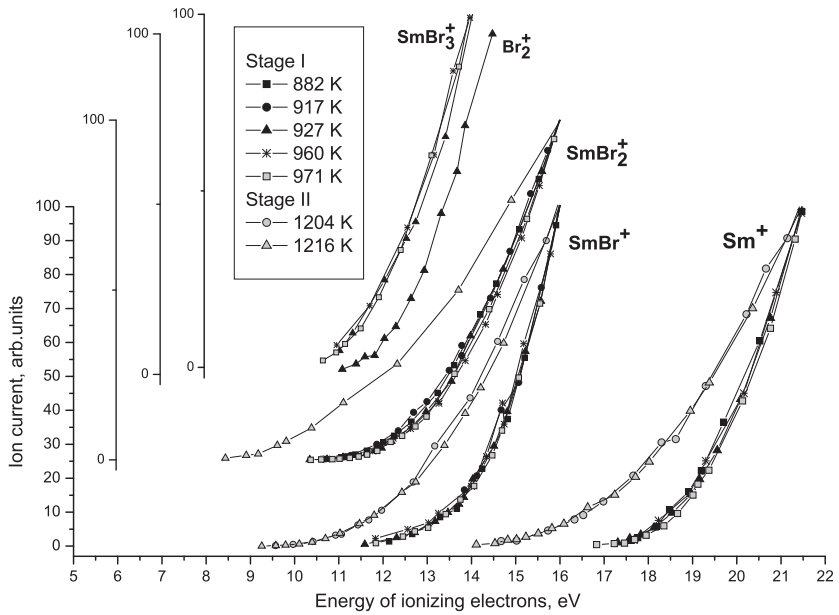

Figure 4. Ionization efficiency curves at stages I and II of vaporization of $SmBr_3$.

Ytterbium, samarium, and europium dibromides

The ion currents of the species recorded on heating in EI mass spectra are summarized in Table 1. The ion current ratios are shown in Figs. 5, 6, and 7 for $YbBr_2$, $SmBr_2$, and $EuBr_2$, respectively. The observation of $YbBr_3^+$ and $SmBr_3^+$ ions in the spectra indicates the presence of the $LnBr_3$ molecules which are formed, in our opinion, by the disproportionation of the dibromides according to reaction (2). It is noteworthy that the mass spectra of the Yb and Sm dibromides are quite similar to those of the corresponding tribromides at stage II.

It can be seen from Fig. 5 that the slope of the $I(Yb^+)/I(YbBr_2^+)$ curve changes significantly around 1030 K. Such a behavior reflects the competition between different contributions to the Yb^+ ion current and follows the change in shape of the Yb^+ IECs (see Fig. 8). These contributions are predominately from Yb atoms and $YbBr_2$ molecules. There are also two contributions to the $YbBr^+$ ion current. The main one comes from $YbBr_2$ and the minor one from YbBr molecules. The fraction of YbBr molecules in the vapor is estimated to be about 0.5%. The situation is similar in the case of $YbBr_2^+$ ions which are mainly formed from $YbBr_2$ molecules and to a much smaller fraction of about 4% from $YbBr_3$ molecules.

The IECs of the ions from $SmBr_2$ (see Fig. 9) are quite similar to those from $YbBr_2$ with the major difference that the Sm^+ ion current shows no temperature dependence. A possible reason might be the lower vapor pressure of metallic Sm than of Yb in the investigated temperature range.

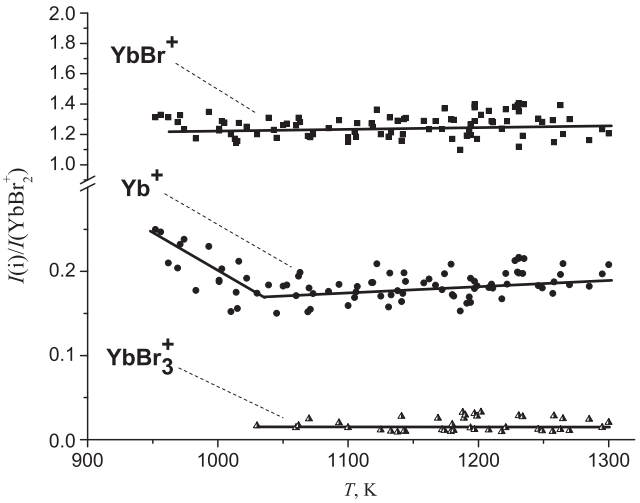

Figure 5. Temperature dependences of the mass spectra upon the vaporization of $YbBr_2$.

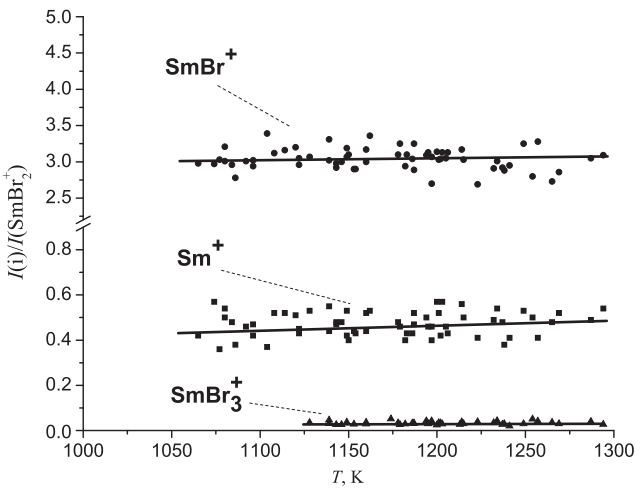

Figure 6. Temperature dependences of the mass spectra upon the vaporization of $SmBr_2$.

The mass spectrum of europium dibromide is distinctly different from those of the ytterbium and samarium dibromides (see Table 1), in that the undetectable $EuBr_3^+$ and $Eu_2Br_4^+$ ions prove the absence of $EuBr_3$ molecules in the vapor within instrumental sensitivity. Accordingly, the decomposition of $EuBr_2$ by reaction (2) is negligible. Nevertheless, the IECs of the Eu^+ and $EuBr^+$ ions demonstrate low-energy tails similar to the other dibromides (see Fig. 10). They correspond to small fractions of gaseous Eu and EuBr, of about 0.05% and 0.3%, respectively.

Vapor composition

The observations described above and our interpretations suggest that the vapor composition of all the investigated bromides is complex. The next stage of data processing therefore involves the separation of the contributions from different molecular precursors to the ion currents. Let us introduce the concept of fragmentation coefficients:

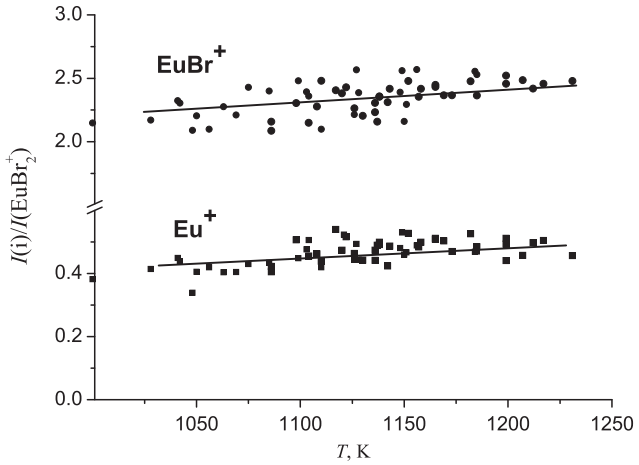

Figure 7. Temperature dependences of the mass spectra upon the vaporization of $EuBr_2$.

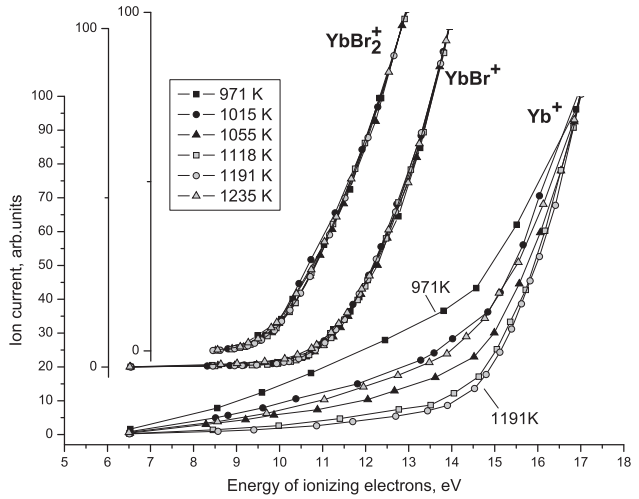

Figure 8. Ionization efficiency curves upon the vaporization of $YbBr_2$.

$$f_{ij} = I_{ij}/I_{jj}, \tag{3}$$

which determine the ratio between the $LnBr_i^+$ fragment and $LnBr_j^+$ molecular ion currents formed from a $LnBr_j$ molecule ($i < j$). The ion currents I_{03}, I_{13}, and I_{23} refer to those of the fragment ions Ln^+, $LnBr^+$, and $LnBr_2^+$ originating from a $LnBr_3$ molecule. Accordingly, I_{33} refers to $LnBr_3^+$ from $LnBr_3$. This results in Eqn. (4) for the fragment ions:

$$I_{i3} = f_{i3} I_{33}, (i = 0, 1, 2). \tag{4}$$

Likewise, for $LnBr_2$ molecules, we obtain the expressions:

$$I_{i2} = f_{i2} I_{22}, (i = 0, 1). \tag{5}$$

Thus, the coefficients f_{03}, f_{13}, f_{23}, f_{02}, and f_{12} attribute the ion currents to molecular precursors. With this in mind, we consider the balance equations of ion currents measured upon vaporization of $LnBr_3$ at stage I:

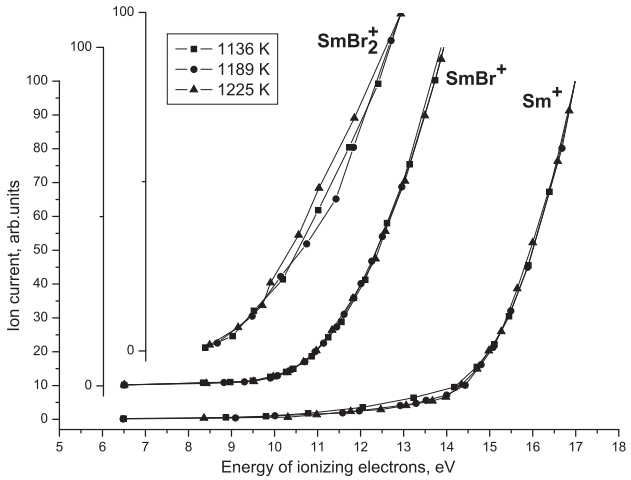

Figure 9. Ionization efficiency curves upon the vaporization of $SmBr_2$.

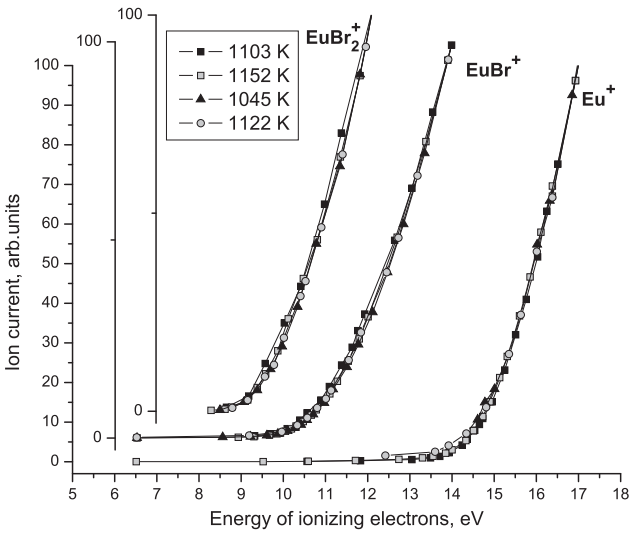

Figure 10. Ionization efficiency curves upon the vaporization of $EuBr_2$.

$$I_2 = I_{22} + f_{23} I_3, \tag{6}$$

$$I_1 = f_{13} I_3 + f_{12} I_{22}, \tag{7}$$

$$I_0 = f_{03} I_3 + f_{02} I_{22}, \tag{8}$$

where I_i is the measured ion current.

Fragmentation coefficients for $LnBr_2$ molecules can be expressed as:

$$f_{12} = \frac{I_1 - f_{13} I_3}{I_2 - f_{23} I_3}, \tag{9}$$

$$f_{02} = \frac{I_0 - f_{03} I_3}{I_2 - f_{23} I_3}. \tag{10}$$

Equations (9) and (10) are valid for each of the experimental data sets at stage I if one neglects the temperature dependence of f_{02} and f_{12}. They can therefore be written for two various temperatures as:

$$f_{02}(T_1) = f_{02}(T_2), \tag{11}$$

$$f_{12}(T_1) = f_{12}(T_2). \tag{12}$$

Then

$$\frac{I'_1 - f_{13} I'_3}{I'_2 - f_{23} I'_3} = \frac{I''_1 - f_{13} I''_3}{I''_2 - f_{23} I''_3}, \tag{13}$$

$$\frac{I'_0 - f_{03} I'_3}{I'_2 - f_{23} I'_3} = \frac{I''_0 - f_{03} I''_3}{I''_2 - f_{23} I''_3}, \tag{14}$$

where I_i' and I_i'' are the ion currents for the first and second random points.

A redundant system of type (13), (14) was devised for the experimental data on ion currents measured at different temperatures, and solved using Mathcad software. The values f_{03}, f_{13}, f_{23}, f_{02}, and f_{12} were found by a least-squares procedure (see Table 2).

The fractions of vapor species (Table 1) were calculated using the relationship:

Table 2. Fragmentation coefficients of $LnBr_2$ and $LnBr_3$ molecules

	Value**	
Coefficient*	Yb	Sm
$f_{02} = I(Ln^+, LnBr_2)/I(LnBr_2^+, LnBr_2)$	0.2 ± 0.1	0.6 ± 0.2
$f_{12} = I(LnBr^+, LnBr_2)/I(LnBr_2^+, LnBr_2)$	1.2 ± 0.2	3.5 ± 0.6
$f_{03} = I(Ln^+, LnBr_3)/I(LnBr_3^+, LnBr_3)$	0.4 ± 0.1	0.7 ± 0.1
$f_{13} = I(LnBr^+, LnBr_3)/I(LnBr_3^+, LnBr_3)$	1.2 ± 0.3	0.5 ± 0.1
$f_{23} = I(LnBr_2^+, LnBr_3)/I(LnBr_3^+, LnBr_3)$	2.0 ± 0.3	5.0 ± 0.5

*The term I(A, B) denotes the intensity of species A formed from species B, e.g. $I(Ln^+, LnBr_2)$ is the intensity of the current of Ln^+ ions formed from $LnBr_2$ molecules.
**Standard deviation follows the ± sign.

$$P_j \sim \frac{T}{\sigma_j} \sum_i \frac{I_i}{\gamma_i a_i}, \quad (15)$$

where p_j is the partial pressure, T is the cell temperature, σ_j^{mol} is the total ionization cross section of the jth molecule with the working energy of ionizing electrons (calculated on the basis of ionization cross sections σ_n^{at} of atoms[22] n using the expression[23] $\sigma_j^{mol} = 0.75\sum_n \sigma_n^{at}$), $\sum_i \frac{I_{ij}}{\gamma_i a_i}$ is the total ion current of ions i of all types formed from molecule j (calculated on the basis of the resultant fragmentation coefficients, Table 2), a_i is the coefficient taking into account the natural abundance of isotopes of the measured ion, and γ_i is the coefficient of ion-electron conversion (it is assumed that $\gamma_i \sim M_i^{-1/2}$,[24] where M_i is the mass of the ion).

Negative ions in the vapor of Yb, Sm, and Eu bromides

The negative ions in the TE mass spectra of Yb, Sm, and Eu bromides are listed in Table 1. If one considers the $LnBr_4^-$ and $LnBr_3^-$ ions as a combination of $LnBr_3$ and $LnBr_2$ molecules and Br^- anions, the relative content of these ions in the vapor may, correspondingly, be used as an additional instrument in the analysis of the molecular constituents of the vapor phase.

In the vaporization of $YbBr_3$ and $SmBr_3$ the $LnBr_4^-$ ions were discovered at stage I. Upon transition to stage II their ion currents dropped drastically (see Fig. 11). This observation confirmed the occurrence of reaction (1) as was inferred above throughout the analysis of neutral vapor moieties. $LnBr_3^-$ ions were seen in small amounts at stage I only in the case of ytterbium tribromide. Their fraction gradually increased towards stage II. The concentrations of $LnBr_3^-$ and $LnBr_4^-$ ions at stage II are of the same order of magnitude and correspond to those observed for the vaporization of $LnBr_2$. These changes in the temperature dependence of negative ion mass spectra are shown in Fig. 11. An additional argument in parallel with the molecular analysis in the $SmBr_3$ case is the detection of $SmBr_3^-$ ions only at stage II ($T > 1200$ K). This is a result of the higher decomposition resistance of $SmBr_3$ than of $YbBr_3$.

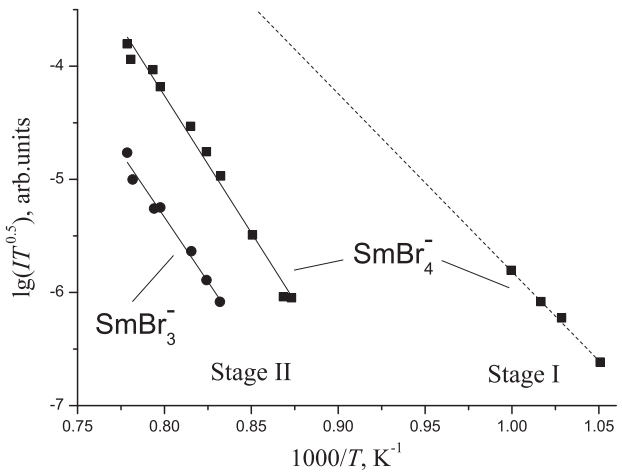

Figure 11. Temperature dependences of the TE mass spectra and their change over time upon the vaporations of $SmBr_3$.

Although there were molecules of ytterbium and samarium monobromides in the vapor, none of the experiments with $LnBr_3$ and $LnBr_2$ revealed the presence of $LnBr_2^-$ ions. Also, these ions were not recorded in additional experiments with $LnBr_2$–Ln systems.

In the case of europium dibromide vaporization only $EuBr_3^-$ ions were recorded. Again this is a confirmation of the above conclusion that the disproportionation of $EuBr_2$ is negligible.

CONCLUSIONS

The vaporization of $SmBr_3$, $YbBr_3$, $SmBr_2$, $EuBr_2$, and $YbBr_2$ was studied in the temperature range of 850–1300 K. The mass spectra were interpreted by the joint analysis of the ionization efficiency functions, the temperature and the time dependences of the ion currents. It was found that only $EuBr_2$ vaporized congruently. In the case of the tribromides, $SmBr_2$ and $YbBr_2$, an initial stage of incongruent vaporization was observed. Various neutral (Ln, Br, Br_2, LnBr, $LnBr_2$, $LnBr_3$, Ln_2Br_4, Ln_2Br_5, and Ln_2Br_6) and charged (Br^-, $LnBr_3^-$, and $LnBr_4^-$) species were detected at different vaporization stages. The quantitative vapor composition of Sm, Eu, and Yb tri- and dibromides was determined. A technique for mass spectra interpretation and accurate determination of the vapor composition of the thermally unstable bromides was developed. This technique is based on a solution of the equations incorporating the fragment ion currents and corresponding fragmentation coefficients. The developed approaches can be extended for characterization of the vaporization of other thermally unstable compounds.

Acknowledgements

This study was supported by The Russian Foundation for Basic Research (project 12-03-31321) and The Ministry of Education and Science of Russian Federation (project 14. B37.21.1192).

REFERENCES

[1] H. Oppermann, P. Schmidt. The thermochemical behaviour of halides, oxidehalides, aluminiumhalides and ammoniumhalides of rare-earth-elements. *Z. Anorg. Allg. Chem.* **2005**, *631*, 1309.
[2] C. Gietmann, G. Gigli, U. Niemann, K. Hilpert. Vaporisation and gas phase chemistry of the rare earth bromides, in *Proc. Ninth International Conference on High Temperature Materials Chemistry*, vol. *97–39*, (Ed: K. E. Spear). The Electrochemical Society, Pennington, **1997**, pp. 657–665.
[3] A. E. Grishin, A. S. Kryuchkov, M. F. Butman, L. S. Kudin, V. B. Motalov, S. N. Nakonechnyi. Sublimation thermodynamics of some lanthanides tribromides, in *Proc. 16th International Conference on Chemical Thermodynamics in Russia*, vol. *I*, ISUCT, Ivanovo, **2007**, pp. 190–191.
[4] R. M. Biefeld, H. A. Eick. Vaporization reactions in the ytterbium-fluorine system. *J. Chem. Phys.* **1975**, *63*, 1190.
[5] T. Petzel, O. Greis. The vaporization behavior of ytterbium (III) fluoride and ytterbium(II) fluoride. *J. Less-Common Met.* **1976**, *46*, 197.

[6] B. Brunetti, A. R. Villani, V. Piacente, P. Scardala. Vaporization study of $YbCl_3$, $YbBr_3$, YbI_2, $LuCl_3$, $LuBr_3$, and LuI_3 and a new assessment of sublimation enthalpies of rare earth trichlorides. *J. Chem. Eng. Data.* **2005**, *50*, 1801.
[7] P. Scardala, A. R. Villani, B. Brunetti, V. Piacente. Vaporization study of samarium trichloride, samarium tribromide and samarium diiodide. *Mater. Chem. Phys.* **2003**, *78*, 637.
[8] A. M. Dunaev, A. S. Kryuchkov, L. S. Kudin, M. F. Butman. Automatic complex for high temperature investigation on basis of mass spectrometer MI1201. *Izv. Vyssh. Uchebn. Zaved. Khim. Khim. Tekhnol.* **2011**, *54*, 73.
[9] A. M. Pogrebnoi, L. S. Kudin, A. Yu. Kuznetsov, M. F. Butman. Molecular and ionic clusters in saturated vapor over lutetium trichloride. *Rapid Commun. Mass Spectrom.* **1997**, *11*, 1536.
[10] G. Meyer, M. S. Wickleder. *Handbook on the Physics and Chemistry of Rare Earths*, vol. *28*, Elsevier, Amsterdam, **2000**, chap. 177.
[11] G. Meyer. The ammonium chloride route to anhydrous rare earth chlorides – The example of YCl_3. *Inorg. Synth.* **1989**, *25*, 146.
[12] G. Meyer. Reduced halides of the rare-earth elements. *Chem. Rev.* **1988**, *88*, 93.
[13] W. H. Zachariasen. Crystal chemical studies of the 5f-series of elements. I. New structure types. *Acta Crystallogr.* **1948**, *1*, 265.
[14] D. Brown, S. Fletcher, D.G. Holah. The preparation and crystallographic properties of certain lanthanide and actinide tribromides and tribromide hexahydrates. *J. Chem. Soc. A* **1968**, 1889.
[15] H. Bärnighausen. Kristallchemische Studien an seltenerd-dihalogeniden die Kristallstruktur von Europium(II)-chlorid. *Rev. Chim. Miner.* **1973**, *10*, 77.
[16] J. M. Haschke, H. A. Eick. The preparation and some properties of europium bromides and hydrated bromides. *J. Inorg. Nucl. Chem.* **1970**, *32*, 2153.
[17] W. Bossert. Untersuchungen zur Struktur und Polymorphie der Dibromide des Dysprosiums, Thuliums und Ytterbiums sowie des Calciums. *PhD thesis*, University of Karlsruhe, Germany, **1981**.
[18] M. F. Butman, L. S. Kudin, V. B. Motalov, D. E. Vorob'ev, A. E. Grishin, A. S. Kryuchkov, K. W. Krämer. A mass spectrometric study of the sublimation of lutetium tribromide under Knudsen and Langmuir conditions. *Russ. J. Phys. Chem. A* **2008**, *82*, 535.
[19] M. F. Butman, V. B. Motalov, L. S. Kudin, A. E. Grishin, A. S. Kryuchkov, K. W. Krämer. A mass spectrometric study of the molecular and ionic sublimation of lanthanum tribromide. *Russ. J. Phys. Chem. A* **2008**, *82*, 164.
[20] L. S. Kudin, M. F. Butman, V. B. Motalov, A. E. Grishin, A. S. Kryuchkov, G. A. Bergman. The thermodynamic parameters of monomer and dimer molecules of cerium and praseodymium tribromides. *High Temp.* **2008**, *46*, 350.
[21] *NIST Chemistry WebBook, NIST Standard Reference Database Number 69*, (Eds: P. J. Linstrom, W. G. Mallard). National Institute of Standards and Technology, Gaithersburg MD, **2013**. Available: http://webbook.nist.gov.
[22] J. B. Mann, in Recent Developments in Mass Spectrometry, *Proceedings of the Conference on Mass Spectrometry, Tokyo*, (Eds: K. Ogata, T. Hayakawa), University Park Press, Baltimore, **1970**, pp. 814–819.
[23] G. V. Belov, V. S. Iorish, V. S. Yungman. Ivtanthermo for windows – database on thermodynamic properties and related software. *CALPHAD: Comput. Coupling Phase Diagrams Thermochem.* **1999**, *23*, 173.
[24] J. Drowart, C. Chatillon, J. Hastie, D. Bonnell. High-temperature mass spectrometry: instrumental techniques, ionization cross-sections, pressure measurements, and thermodynamic data (IUPAC technical report). *Pure Appl. Chem.* **2005**, *77*, 683.

